Suppression of the spontaneous emission of atoms and molecules

Einat Frishman and Moshe Shapiro
Department of Chemical Physics, The Weizmann Institute of Science, Rehovot 76100, Israel
(Received 2 September 2002; published 19 September 2003)

We present an experimentally viable approach for suppressing the spontaneous emission in several atomic and molecular systems. We have shown [E. Frishman and M. Shapiro, Phys. Rev. Lett. **87**, 253001 (2001)] that a coherent excitation of overlapping resonances followed by the application of infrequent interruptions can result in complete suppression of spontaneous emission. In the present work, the overlapping resonances result from splitting a single resonance with an external (spectator) field. An optimized superposition of the two components is formed by a shaped pulse excitation from the ground state.

DOI: 10.1103/PhysRevA.68.032717 PACS number(s): 32.80.Qk, 33.80.−b, 33.70.Ca

I. INTRODUCTION

The possibility of suppressing spontaneous emission has been a source of great interest in recent years [1–9]. In a recent publication [10] we have proposed a new method of completely suppressing spontaneous emission utilizing the interference between resonances. It turns out that the same method is applicable to any decay process, provided it is governed by overlapping resonances.

The method is based on the fact that one can excite coherently a set of overlapping resonances such that their decay exhibits a steplike behavior: the system starts in a quiescent period in which no spontaneous emission occurs, followed by a ''photon burst'' in which spontaneous emission is greatly accelerated, followed by another quiescent period, etc. The quiescent period (and subsequent photon bursts) is due to destructive and constructive interferences between the overlapping resonances. The reason it is impossible to suppress the decay over all times in this fashion is that the phase and magnitude relations that guarantee at a given time the suppression of decay, change as the system evolves in time, until at a certain time point the interference for decay becomes constructive and the system experiences the ''photon burst.''

In order to achieve suppression of decay at all times, we then suggested irradiating the system before it reaches the photon-burst phase by an external laser field which reshuffles the phases of the coefficients of the superposition of overlapping resonances. For the two overlapping resonances case this pulse is simply a π pulse which inverts the populations between levels, thereby effectively sending the system ''backwards'' in time into the quiescent period. Additional external pulses (''interruptions'') must be applied periodically just before the system reaches the photon-burst phases as it moves backwards and forwards in time. In this way the system is forced to forever live on the quiescent period ledge.

In the present paper we further develop this method by lifting the restriction of the pre-existence of overlapping resonances and show that we can suppress the decay of any system, even that of a *single* decaying resonance. This is achieved by (Autler-Townes) splitting [11] a given decaying state into two overlapping field-dressed resonances using an external cw field. We computationally apply this method to show that we can suppress the decay of a variety of realistic atomic [e.g., H($2p$) and Pb($6p7s\,^3P_1^0$)] and molecular [e.g., $Na_2(A\,^1\Sigma_u^+)$] excited states.

II. THEORETICAL FRAMEWORK

A. Elements of the theory of multichannel overlapping resonances

In this section we briefly review the elements of ''partitioning'' theory [12–16] used in the remainder of this paper to treat the interference between overlapping resonances.

Assuming that we have a situation in which bound states interact with continuum states, we define two projection operators Q and P, satisfying the equalities $QQ=Q$, $PP=P$, $PQ=QP=0$, $P+Q=I$, where I is the identity operator. The Q and P operators are chosen to project out the subspaces $\mathcal{Q}$ and $\mathcal{P}$ spanned by bound states and continuum states, respectively.

The full scattering incoming states $|E,\mathbf{n}^-\rangle$ are eigenstates of the Schrödinger equation, written as

$$[E-i\epsilon-H]|E,\mathbf{n}^-\rangle=0, \tag{1}$$

where the $-i\epsilon$ serves to remind us of the incoming boundary conditions. Using the completeness and orthogonality of P and Q, we insert $P+Q$ to the left of $|E,\mathbf{n}^-\rangle$; we then operate on it with P and operate on it separately with Q to obtain the two coupled equations,

$$[E-i\epsilon-PHP]P|E,\mathbf{n}^-\rangle=PHQ|E,\mathbf{n}^-\rangle, \tag{2}$$

$$[E-i\epsilon-QHQ]Q|E,\mathbf{n}^-\rangle=QHP|E,\mathbf{n}^-\rangle. \tag{3}$$

We define two basis sets $|E,\mathbf{n}\rangle$ and $|\alpha\rangle$, which are the solutions of the *homogeneous* (decoupled) parts of Eq. (3), that is,

$$[E-i\epsilon-PHP]|E,\mathbf{n}\rangle=0, \tag{4}$$

$$[E_\alpha-QHQ]|\alpha\rangle=0. \tag{5}$$

Implicit in Eqs. (4) and (5) is that $|E,\mathbf{n}\rangle\in\mathcal{P}$ and $|\alpha\rangle\in\mathcal{Q}$ and as such they are orthogonal to one another. We, in fact, as-

sume that each basis set spans the entire subspace to which it belongs, hence we can write an explicit representation of Q and P as

$$Q=\sum_{\alpha} |\alpha\rangle\langle\alpha|, \tag{6}$$

$$P=\sum_{\mathbf{n}} \int dE|E,\mathbf{n}\rangle\langle E,\mathbf{n}|. \tag{7}$$

Following Fano [14] we can use Eqs. (6) and (7) to write $|E,\mathbf{n}^-\rangle=[P+Q]|E,\mathbf{n}^-\rangle$ in terms of Q and P as

$$|E,\mathbf{n}^-\rangle=\sum_{\alpha} |\alpha\rangle\langle\alpha|E,\mathbf{n}^-\rangle + \sum_{\mathbf{n}'} \int dE'|E',\mathbf{n}'\rangle\langle E',\mathbf{n}'|E,\mathbf{n}^-\rangle. \tag{8}$$

We now solve for $P|E,\mathbf{n}^-\rangle$ by writing it as a sum of the homogeneous solution of Eq. (4) and a particular solution of Eq. (2) obtained by inverting $(E-i\epsilon-PHP)$,

$$P|E,\mathbf{n}^-\rangle=P|E,\mathbf{n}\rangle+[E-i\epsilon-PHP]^{-1}PHQ|E,\mathbf{n}^-\rangle. \tag{9}$$

Substituting this solution into Eq. (3), we obtain that

$$[E-i\epsilon-Q\mathcal{H}(E)Q]Q|E,\mathbf{n}^-\rangle=QHP|E,\mathbf{n}\rangle, \tag{10}$$

where

$$Q\mathcal{H}(E)Q\equiv QHQ+QHP[E-i\epsilon-PHP]^{-1}PHQ. \tag{11}$$

Finally, by inversion of $[E-i\epsilon-Q\mathcal{H}(E)Q]$ we get

$$Q|E,\mathbf{n}^-\rangle=[E-i\epsilon-Q\mathcal{H}(E)Q]^{-1}QHP|E,\mathbf{n}\rangle, \tag{12}$$

which involves only the Q projection of the full scattering states $|E,\mathbf{n}^-\rangle$.

B. Photon-matter resonances

In a previous publication [10] we showed how to take advantage of the presence of *overlapping* resonances to delay and even suppress general decay processes. The issue we raise in the present paper is what to do when the resonances are so far apart that they are in fact *isolated*. We show that under these circumstances it is still possible to use our past methodology [10] by splitting each isolated resonance into two. This is done by radiatively coupling each isolated resonance to a lower-lying nondecaying level.

We thus consider an isolated resonance $|a\rangle$ which acquires its width due to spontaneous emission to a manifold of lower-lying states denoted as $|\gamma\rangle$. In order to (Autler-Townes [11]) split this resonance we couple it to a lower-lying state $|b\rangle$ using a monochromatic source of frequency ω_i. The situation is described in Fig. 1.

The total Hamiltonian assumes the form

$$H=H_M+H_R+H_{MR}, \tag{13}$$

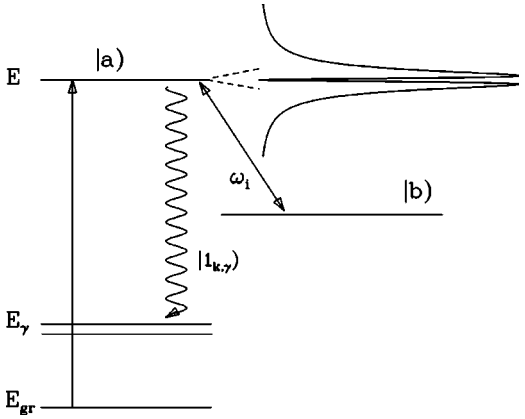

FIG. 1. The energy levels and spontaneous emission pathways of an Autler-Townes split resonance. Shown is a resonance $|a\rangle$ of energy E_a, coupled by a monochromatic light of frequency ω_i to a lower-lying state $|b\rangle$. As a result of this coupling, the resonance splits, displaying a hole at the center of the absorption line at $E=E_a$. The wiggly line represents spontaneously emitted photons to lower-lying states of energies E_γ. Also shown is the ground state of energy E_{gr} which is excited, using a shaped pulse, to form a superposition of the split components of $|a\rangle$ such that the decay is delayed.

where H_M is the matter Hamiltonian, H_R is the radiative Hamiltonian, and H_{MR} is the matter-radiation interaction. For the two material levels $|a\rangle$ and $|b\rangle$ we write H_M as

$$H_M=\tfrac{1}{2}\hbar\omega_{a,b}\sigma_z, \tag{14}$$

where $\omega_{a,b}\equiv(E_a-E_b)/\hbar$ and

$$\sigma_z|a\rangle=|a\rangle, \quad \sigma_z|b\rangle=-|b\rangle. \tag{15}$$

The free radiative Hamiltonian is written as

$$H_R=\sum_{\mathbf{k}} \hbar\omega_k\left[a_{\mathbf{k}}^\dagger a_{\mathbf{k}}+\frac{1}{2}\right]. \tag{16}$$

The $|a\rangle|0,\ldots,0,n_i,0,\ldots,0\rangle$ state, denoted for simplicity as $|a,n_i,0\rangle$, and the $|b\rangle|0,\ldots,0,n_i+1,0,\ldots,0\rangle$ state, denoted for simplicity as $|b,n_i+1,0\rangle$, are eigenstates of H_0, the uncoupled Hamiltonian, defined as $H_0=H_M+H_R$. Fixing the zero of energy to be midway between E_a and E_b, we have that

$$H_0|a,n_i,0\rangle=\left(E_{n_i}+\frac{1}{2}\hbar\Delta\right)|a,n_i,0\rangle,$$

$$H_0|b,n_i+1,0\rangle=\left(E_{n_i}-\frac{1}{2}\hbar\Delta\right)|b,n_i+1,0\rangle, \tag{17}$$

where $E_{n_i}\equiv n_i\hbar\omega_i+\frac{1}{2}\hbar\omega_{a,b}-\frac{1}{2}\hbar\Delta$ with $\Delta\equiv\omega_{a,b}-\omega_i$, being the energy of these states relative to the vacuum energy.

The matter-radiation Hamiltonian within the dipole approximation is given as

$$H_{MR}=-\mathbf{d}\cdot\boldsymbol{\epsilon}_{\mathbf{L}}(R), \tag{18}$$

where

$$\mathbf{d}=\mathbf{d}_{ab}(\sigma_+ + \sigma_-),$$

$$\boldsymbol{\epsilon}_L(R)=\sqrt{\frac{\hbar\omega_i}{2\varepsilon_0 V}}\boldsymbol{\epsilon}_L(a+a^\dagger). \tag{19}$$

H_{MR} applies only to the part of the matter radiation due to the external laser field and does not include the coupling of the vacuum to the one-photon states in other modes that brings about spontaneous emission—this coupling will be dealt with separately below [Eq. (28)].

Neglecting nonresonant coupling (i.e., rotating wave approximation), we obtain that

$$H_{MR}=\hbar g_i(\sigma_+ a + a^\dagger \sigma_-). \tag{20}$$

Taking the Q operator as

$$Q\equiv|a,n_i,0\rangle\langle a,n_i,0|+|b,n_i+1,0\rangle\langle b,n_i+1,0|, \tag{21}$$

we have that (in matrix form for basis functions $|a,n_i,0\rangle$ and $|b,n_i+1,0\rangle$)

$$\underline{\underline{\mathrm{QHQ}}}=\begin{pmatrix} E_{n_i}+\frac{1}{2}\hbar\Delta & \hbar g_i\sqrt{n_i+1} \\ \hbar g_i\sqrt{n_i+1} & E_{n_i}-\frac{1}{2}\hbar\Delta \end{pmatrix}, \tag{22}$$

where

$$g_i=-\sqrt{\frac{\hbar\omega_i}{2\varepsilon_0 V}}\frac{\boldsymbol{\epsilon}_L\cdot\mathbf{d}_{ab}}{\hbar}.$$

The eigenvalues of $\underline{\underline{\mathrm{QHQ}}}$ are given as

$$E^{\pm}_{n_i}=E_{n_i}\pm\frac{1}{2}\hbar\Omega_{n_i}, \tag{23}$$

where $\Omega^2_{n_i}=\Delta^2+4g_i^2(n_i+1)$. The (''dressed'') eigenstates corresponding to these eigenvalues are given [18] as

$$|+n_i,0\rangle=\sin\theta|b,n_i+1,0\rangle+\cos\theta|a,n_i,0\rangle,$$

$$|-n_i,0\rangle=\cos\theta|b,n_i+1,0\rangle-\sin\theta|a,n_i,0\rangle, \tag{24}$$

where $\tan 2\theta=-\Omega_i/\Delta$, $\hbar\Omega_i\equiv-\mathbf{d}_{ab}\cdot\mathcal{E}_i$, and

$$\boldsymbol{\mathcal{E}}_i\equiv 2\boldsymbol{\epsilon}_L\sqrt{\frac{n_i\hbar\omega_i}{2\varepsilon_0 V}}. \tag{25}$$

The two orthogonal states $|+n_i,0\rangle$, $|-n_i,0\rangle$ of the Q manifold and the states $|E,m_i,\beta\rangle$ of the P manifold satisfy,

$$\langle\alpha',n_i',0|QHQ|\alpha,n_i,0\rangle=E_\alpha\delta_{n_i',n_i}\delta_{\alpha',\alpha}, \tag{26}$$

where $\alpha,\alpha'=\pm$, and

$$\langle E',m_i',\beta'|PHP|E,m_i,\beta\rangle=(E+m_i\hbar\omega_i)\,\delta(E'-E)\,\delta_{m_i',m_i}\delta_{\beta',\beta}. \tag{27}$$

The $|\beta\rangle$ state of the above is a combined material state γ and a (spontaneously emitted) one-photon state in the $\hat{\mathbf{k}}$ direction and $\hat{\boldsymbol{\epsilon}}$ polarization.

The excited $|a,n_i,0\rangle$ state emits a photon and decays into the P space, with the ω_i photons acting as spectators [19], which means that their number does not change in the process.

Denoting the matter-radiation matrix elements as

$$V^{(n)}(a,0|E,\beta)\equiv\langle a,n,0|QHP|E,n,\beta\rangle,$$

and analogously for state b, we have that

$$V^{(n,m)}(+,0|E,\beta)=(\sin\theta)V^{(n+1)}(b,0|E,\beta)\,\delta_{n+1,m}+(\cos\theta)V^{(n)}(a,0|E,\beta)\,\delta_{n,m},$$

$$V^{(n,m)}(-,0|E,\beta)=(\cos\theta)V^{(n+1)}(b,0|E,\beta)\,\delta_{n+1,m}-(\sin\theta)V^{(n)}(a,0|E,\beta)\,\delta_{n,m}, \tag{28}$$

where we have for brevity denoted n_i as n. Each state $|\beta\rangle$ may be only coupled to one of the two opposite-symmetry states $|a\rangle$ and $|b\rangle$. Assuming that the lower lying $|b,n_i+1,0\rangle$ state is a nondecaying (or slowly decaying) state, we may omit the terms with $V^{(n+1)}(b,0|E,\beta)$ from Eq. (28).

The fully interacting $|E,n,\beta^-\rangle$ states, obtained from Eq. (8), form a complete basis set and can be used to expand $|\Psi(t)\rangle$, the full time dependent wavefunction. Assuming that initially (at $t=0$) we populate a superposition of zero-photon states and a coherent state in the ω_i mode,

$$|\Psi(t=0)\rangle=\sum_{\alpha,n}c_{\alpha,n}|\alpha,n,0\rangle, \tag{29}$$

where $c_{\alpha,n}=c_\alpha c_n$, with $c_n=x^n/n!$ $(x\gg 1)$, the wave function at time t is given by

$$|\Psi(t)\rangle=\sum_{\alpha,n}\sum_{\beta,m}c_{\alpha,n}\int_{E_i}^{E_f}dE e^{-iEt/\hbar}|E,m,\beta^-\rangle\times\langle E,m,\beta^-|\alpha,n,0\rangle. \tag{30}$$

Applying Eq. (12) to the present case we obtain that $a^{(n,m)}_{\alpha,\beta}(E)$ the amplitude function is given as

$$a^{(n,m)}_{\alpha,\beta}(E)\equiv\langle\alpha,n,0|E,m,\beta^-\rangle=\sum_{\alpha',n'}\langle\alpha,n,0|[E-i\epsilon-Q\mathcal{H}(E)Q]^{-1}|\alpha',n',0\rangle\times\langle\alpha',n',0|QHP|E,m,\beta\rangle, \tag{31}$$

where $Q\mathcal{H}(E)Q$ is defined in Eq. (11). Using the well-known identity $(E-i\epsilon-PHP)^{-1}=\mathrm{P}(E-PHP)^{-1}+i\pi\delta(E-PHP)$, with P denoting a Cauchy principal value integral, we can write the matrix elements of $Q\mathcal{H}(E)Q$ as

$$\langle \alpha,n,0|Q\mathcal{H}(E)Q|\alpha',n',0\rangle = \left[E_\alpha \delta_{\alpha,\alpha'} + \hbar \Delta^{(n)}_{\alpha,\alpha'}(E) + i\frac{\hbar}{2}\Gamma^{(n)}_{\alpha,\alpha'}(E)\right]\delta_{nn'}, \tag{32}$$

where

$$\Gamma^{(n)}_{\alpha,\alpha'}(E) \equiv \frac{2\pi}{\hbar}\sum_{\beta,m} V^{(n,m)}(\alpha|E,\beta)V^{(n,m)}(E,\beta|\alpha'),$$

$$\Delta^{(n)}_{\alpha,\alpha'}(E) \equiv \frac{1}{2\pi}\mathrm{P}\int_{E_i}^{E_f} dE' \frac{\Gamma^{(n)}_{\alpha,\alpha'}(E')}{E-E'}. \tag{33}$$

Operating on Eq. (30) with $\langle \alpha',n',0|$, we obtain that the amplitudes of the $|\alpha',n',0\rangle$ states at time t equal,

$$\langle \alpha',n',0\ |\Psi(t)\rangle = \sum_{\alpha,n} c_{\alpha,n}\int_{E_i}^{E_f} dE e^{-iEt/\hbar} = \sum_{\beta,m}\langle \alpha',n',0|E,m,\beta^-\rangle\langle E,m,\beta^-|\alpha,n,0\rangle = \sum_{\alpha} c_{\alpha,n} M^{(n)}_{\alpha'\alpha}(t), \tag{34}$$

where

$$M^{(n)}_{\alpha'\alpha}(t) = \sum_{\beta,m}\int_{E_i}^{E_f} dE e^{-iEt/\hbar} a^{(n,m)}_{\alpha',\beta}(E) a^{(n,m)*}_{\alpha,\beta}(E). \tag{35}$$

We note that since a state $|\beta\rangle$ may either be coupled to $|a\rangle$ or to $|b\rangle$, only the $n=n'$ terms of Eq. (34) are nonvanishing.

The total population in the zero-photon material states with n spectator photons in the ith mode, at time t, $P^{(n)}(0,\mathbf{c},t)$, is given by

$$P^{(n)}(0,\mathbf{c},t) = \sum_{\alpha} |\langle \alpha,n,0|\Psi(t)\rangle|^2, \tag{36}$$

where $\mathbf{c}\equiv\{c_{\alpha,n}\}$.

In order to delay the decay we need to find the set of initial coefficients $\mathbf{c}$ which maximizes $P^{(n)}(0,\mathbf{c},t)$ at a given time τ after preparation. Once such a set of coefficients is found, the overlapping resonances thus populated exhibit a steplike decay pattern [10], a sample of which is shown in Fig. 5. Basically, after a quiescent period in which a photon emitted by one resonance gets immediately reabsorbed by another, the system undergoes a period of rapid decay in which a burst of photons escapes the atom. The photon burst phase is followed by another quiescent phase, etc.

The delay in the emission afforded by the quiescent phase may be of great practical importance for many laser applications by itself. However, we usually want to go one step further and suppress the emission at all times. As shown previously [10] it is possible to do so in the 2×2 case by applying a π pulse at, or close to, the end of the quiescent period. The effect of the π pulse which transforms the system according to the transformation matrix

$$\begin{pmatrix} 0 & i \\ i & 0 \end{pmatrix},$$

is to interchange the populations between the two levels. Such an interchange of population in a two level system is known to effectively reverse the direction of time. As a result, after the application of the π pulse, the system moves away from the onset of the photon burst phase until it reaches the $-\tau$ time, at which point another photon burst is about to be launched. We avoid such a burst by applying another π pulse which reverses the flow of time once again, sending the system back in the positive time sense. We continue applying a π pulse every 2τ interval, thus confining the system forever to the quiescent phase, making it shuttle back and forth between $-\tau$ and τ. As shown, e.g., in Fig. 5, to be discussed in greater detail below, spontaneous emission is thereby effectively blocked. The above analysis also applies to the $N_\alpha > 2$ case, where the transformation is slightly more complicated [10].

We now turn our attention to the application of the above strategy for the Autler-Townes split resonance case. The radiative couplings to the $\beta=\gamma,\mathbf{k},\hat{\boldsymbol{\epsilon}}$ mode, where $\omega_{\mathbf{k},\gamma} = (E-E_\gamma)/\hbar$, are [20]

$$\langle q,n_i,0|QHP|\mathbf{k},\hat{\boldsymbol{\epsilon}},\gamma,n_i\rangle = \begin{cases} ie\sqrt{\dfrac{\hbar\omega_{\mathbf{k},\gamma}}{2\varepsilon_0 V_0}}\hat{\boldsymbol{\varepsilon}}_{\mathbf{k},\hat{\boldsymbol{\epsilon}}}\cdot\mathbf{D}_{q,\gamma}, & E > E_\gamma + n_i\hbar\omega_i \\ 0, & \text{otherwise,} \end{cases} \tag{37}$$

where $q=a,b$ and

$$|E,n_i,\beta\rangle \equiv |E,n_i,\hat{\mathbf{k}},\hat{\boldsymbol{\epsilon}},\gamma\rangle = \frac{k}{\sqrt{\hbar c}}|\mathbf{k},\hat{\boldsymbol{\epsilon}},\gamma,n_i\rangle.$$

We note that the dipole matrix elements for spontaneous emission do not depend on the number of ω_i spectator photons (but the total energy includes it).

Integrating over the directions $\hat{\mathbf{k}}$ of emission of the photons and summing over the two possible photon polarization directions $\hat{\boldsymbol{\epsilon}}$, we obtain that

$$\Gamma^{(n)}_{qq'}(E) = \frac{e^2}{3\pi\varepsilon_0\hbar^4 c^3}\sum_{\{\gamma:E>E_\gamma+n\hbar\omega_i\}}\mathbf{D}_{q,\gamma}\cdot\mathbf{D}^*_{q',\gamma} \times (E-E_\gamma-n\hbar\omega_i)^3. \tag{38}$$

The level shifts $\Delta^{(n)}_{qq'}(E)$ can be calculated from $\Gamma^{(n)}_{qq'}(E)$ using Eq. (33).

The decay matrix elements in the dressed-state basis (dropping the energy argument for brevity) can be expressed in the $|a\rangle$, $|b\rangle$ basis as

$$\Gamma_{++}(\theta)=(\sin^2\theta)\Gamma_{bb}+(\cos^2\theta)\Gamma_{aa}+(\sin 2\theta)\mathrm{Re}[\Gamma_{ab}],$$

$$\Gamma_{--}(\theta)=(\cos^2\theta)\Gamma_{bb}+(\sin^2\theta)\Gamma_{aa}-(\sin 2\theta)\mathrm{Re}[\Gamma_{ab}],$$

$$\Gamma_{+-}(\theta)=\frac{1}{2}(\sin 2\theta)(\Gamma_{bb}-\Gamma_{aa})+(\cos 2\theta)\mathrm{Re}[\Gamma_{ab}]+i\,\mathrm{Im}[\Gamma_{ab}]. \tag{39}$$

Since the bare states $|a\rangle$ and $|b\rangle$ have *opposite symmetries*, they emit into different sets of levels, resulting in $\Gamma_{ab}=0$. Therefore the above expressions can be written as

$$\Gamma_{++}(\theta)=\overline{\Gamma}-(\cos 2\theta)\hat{\Gamma},$$

$$\Gamma_{--}(\theta)=\overline{\Gamma}+(\cos 2\theta)\hat{\Gamma}, \tag{40}$$

$$\Gamma_{+-}(\theta)=(\sin 2\theta)\hat{\Gamma},$$

where $\overline{\Gamma}=\frac{1}{2}(\Gamma_{aa}+\Gamma_{bb})$ and $\hat{\Gamma}=\frac{1}{2}(\Gamma_{bb}-\Gamma_{aa})$.

We envision the coupling laser leading to the Autler-Townes splitting to be in the IR, for which fluorescence lifetimes are in the millisecond range, whereas the emission we propose to suppress occurs on the 10 ns range, i.e., a difference of five orders of magnitude, hence the neglect of the IR fluorescence over the time scales of interest in this paper is completely justified.

The possibility of delaying the spontaneous emission is governed by the ratio

$$f_1(E,\theta)\equiv\frac{|\Gamma_{+-}(E)|}{[\Gamma_{++}(E)\Gamma_{--}(E)]^{1/2}}, \tag{41}$$

which (due to the Schwartz inequality) can assume values between 0 and 1. The unity value leads to maximal delay and the null value to the complete loss of control over spontaneous emission. The ratio reaches its maximum value when $\theta=\pi/4$, i.e., when the field is on-resonance. It then equals

$$f_1(\pi/4)=\frac{|\Gamma_{bb}-\Gamma_{aa}|}{\Gamma_{aa}+\Gamma_{bb}}=\left|\frac{\Gamma_{aa}}{\overline{\Gamma}}-1\right|. \tag{42}$$

The steplike nature of the decay pattern becomes more and more pronounced as this ratio increases. This is because this ratio reflects the relative magnitude of the off-diagonal elements $\Gamma_{aa'}$ with respect to the diagonal ones. If the off-diagonal elements are zero (or small) the ''control matrix,'' whose eigenvalues we calculate [see Eqs. (34)–(36) and Ref. [10]] will be diagonal (or near diagonal) and no active control is possible.

The maximal degree of delay of the spontaneous emission is attained when $\Gamma_{bb}\approx 0$, i.e., the $|b\rangle$ state is a meta-stable excited state; in that case $\Gamma_{++}(E)=\Gamma_{--}(E)=|\Gamma_{--}(E)|=\frac{1}{2}\Gamma_{aa}(E)$.

The ability to control the spontaneous emission resulting from the introduction of the cw field is demonstrated below.

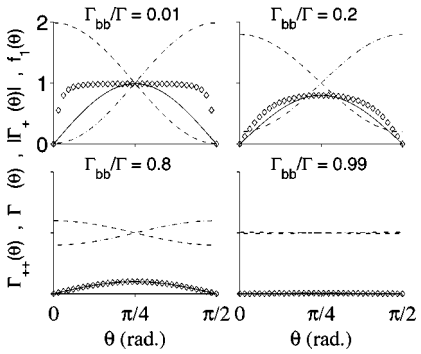

FIG. 2. Γ_{++} (dashed), Γ_{--} (dot-dashed), $|\Gamma_{+-}|$ (solid) (all in units of $\overline{\Gamma}$) and $f\equiv|\Gamma_{+-}|/(\Gamma++\Gamma_{--})^{1/2}$ ($\diamond$).

In all the discussion below we assume that the energy dependence of the widths $\Gamma^{(n)}_{qq'}(E)$ can be neglected over the integration range, which is of the order of magnitude of the width itself. In Fig. 2 we show Γ_{++}, Γ_{--}, $|\Gamma_{+-}|$, and f_1 which result from the introduction of a cw coupling field as a function of the mixing angle θ. The results are shown for several different values of $\Gamma_{bb}/\overline{\Gamma}$.

In Fig. 2(a), $\Gamma_{bb}/\overline{\Gamma}=0.01$, which means that state $|b\rangle$ is a metastable state. The degree of delay of emission we achieve in this case reaches the maximum value it possibly can: $f_1(\theta)\approx 1$. This degree of control is maintained over a wide range of the mixing angle θ. Essentially control is degraded only when the detuning is very large, causing almost no mixing between the $|a\rangle$ and the $|b\rangle$ states ($\theta\approx 0$ or $\theta\approx\pi/2$).

In the next case, shown in Fig. 2(b), $\Gamma_{bb}/\overline{\Gamma}=0.2$. It shows slightly less control, with our ability to delay the decay now being more dependent on the field tuning. The optimal control is achieved, as discussed above, exactly on resonance, where $f_1=0.8$ [see Eq. (42)]. The possibility of control is being completely eliminated as we increase the $\Gamma_{bb}/\overline{\Gamma}$ ratio, as shown in the lower panel of Fig. 2.

Another important control variable is the ratio between Γ_{aa}, the resonance widths, and $\Delta E\equiv|E^+_{n_i}-E^-_{n_i}|=\hbar|\Omega_{n_i}|$, the energy spacings between Autler-Townes split resonances. According to Eq. (23), the Autler-Townes splitting enables the tuning of the energy spacings between the resonances by varying the Rabi frequency Ω_{n_i} of the ''spectator'' cw field. Sample $a^{(n,m)}_{\alpha,\beta}(E)$ amplitudes for overlapping resonances with $\Delta E/(\hbar\Gamma)$ varying between 0.2 and 5 are shown in Fig. 3.

The signature of the interference is the appearance of a ''dark state,'' i.e., a continuum energy where the line shape [equal to $|a^{(n,m)}_{\alpha,\beta}(E)|^2$] dips to zero, occurring at the peaks ($E^+_{n_i}$ or $E^-_{n_i}$) of the neighboring resonance for each line shape. These dark states, first discovered in Ref. [16], bring about the phenomenon of electromagnetically induced transparency [17] hole, midway between the resonances, shown in Fig. 1, for a particular linear combination of the resonances. In the optimized case studied here the $\Sigma_\beta|\Sigma_{\alpha=\pm}c_\alpha a^*_{\alpha,\beta}(E)|^2$ line shapes shown in the lower panel of Fig. 3 do not necessarily dip to zero.

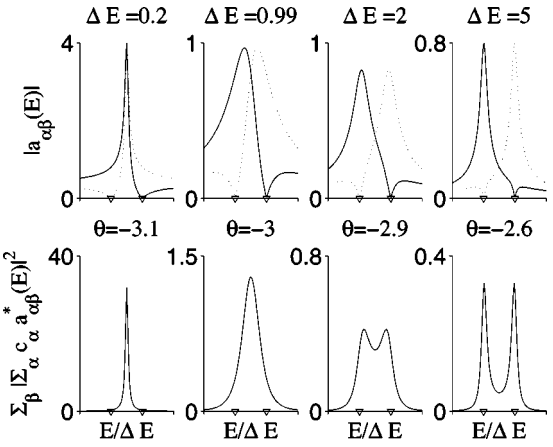

FIG. 3. (Upper panel) The $|a_{\pm,\beta}(E)|$ amplitudes in the 2×2 case, for several values of the levels spacing ΔE for a constant Γ. (ΔE is given in units of $\hbar\Gamma$) The x axis is scaled to encompass $3\Delta E$. The $|a_{+,\beta}(E)|$ [in units of $(\Delta E)^{-1/2}$] is seen to dip to zero at $E^{-}_{n_i}$ and the $|a_{-,\beta}(E)|$ is seen to dip to zero at $E^{+}_{n_i}$. The $E^{\pm}_{n_i}$ positions are denoted by the triangles. Each amplitude is automatically normalized, i.e., they satisfy $\int dE a^{*}_{\alpha\beta}(E)a_{\alpha'\beta}(E)=\delta_{\alpha,\alpha'}$ (upper panel), the same as the lower panel for the $\Sigma_\beta|\Sigma_{\alpha=\pm}c_\alpha a^{*}_{\alpha,\beta}(E)|^2$ line shapes (in units of $(\Delta E)^{-1}$). The optimal initial superposition is in the form $(c_-,c_-e^{i\theta})$, and θ is given below each plot.

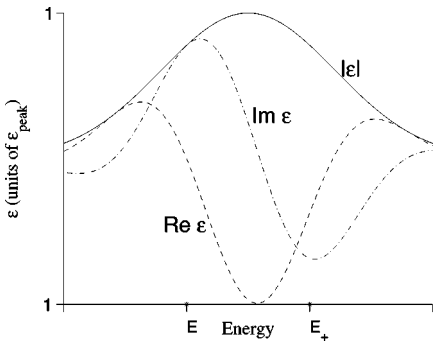

FIG. 4. The light pulse (in frequency space) used to excite the Autler-Townes split $|2P_0\rangle$ state from the ground $1S$ state to produce the optimal c_α coefficients. This choice of coefficients is the one most effective in delaying the emission (in the absence of the interruptions) over the optimization time of 2.4 ns.

III. SUPPRESSION OF SPONTANEOUS EMISSION IN SAMPLE SYSTEMS

A. The hydrogen atom

We first study the suppression of the spontaneous emission of a hydrogen atom in the $|2P_0\rangle$ state, which can only decay to a *single* (the ground $|1S_0\rangle$) state. We do so by coupling the $|2P_0\rangle$ state, which is identified with state $|a\rangle$ of Fig. 1, with the $|3S\rangle$ state (identified with the $|b\rangle$ state of that figure) using a resonant cw field. Contrary to Fig. 1, here $E_b>E_a$, which means that $\Gamma_{bb}\neq0$.

All the parameters needed for this case are known analytically. Thus, the energy differences between the material states are $E_{2P}-E_{1S}=\frac{3}{4}me^4/[2\hbar^2(4\pi\varepsilon_0)^2]=\frac{3}{8}$ a.u., and $E_{3S}-E_{2P}=\frac{5}{72}$ a.u. We obtain that

$$\Gamma_{2P_0,2P_0}(E)=\frac{2^{15}}{3^{11}}\frac{4\pi\varepsilon_0}{m^2e^2c^3}[E-E_{1S}-(n_i+1)\hbar\omega_i]^3$$
$$=626.8\ \mu s^{-1},$$

$$\Gamma_{3S,3S}(E)=3\times\frac{2^{15}\times3^6}{5^{12}}\frac{4\pi\varepsilon_0}{m^2e^2c^3}(E-E_{2P}-n_i\hbar\omega_i)^3$$
$$=6.32\ \mu s^{-1}. \quad (43)$$

The corresponding lifetimes are $\tau_{2P_0}=1.586$ ns and $\tau_{3S}=157.4$ ns. Using Eq. (40), we obtain for the on-resonance Autler-Townes split states $|\pm,n\rangle=(|2P,n+1\rangle\pm|3S,n\rangle)/\sqrt{2}$, that $\Gamma_{++}(E)=\Gamma_{--}(E)=316.6\ \mu s^{-1}$ and $|\Gamma_{+-}(E)|=310.2\ \mu s^{-1}$.

Delaying the spontaneous emission is achieved by exciting the ground-state hydrogen atom with a light pulse (linearly polarized in the x direction) whose shape, as determined according to the procedure outlined in the preceding section, for an optimization time of 2.4 ns, is shown in Fig. 4.

The result of exciting with an optimized pulse (a sample of which is given in Fig. 4) is displayed in Fig. 5 for four different splittings (ΔE). We see a steplike decay: the system starts with a quiescent period which lasts longer and longer the smaller the Autler-Townes splitting (i.e., Ω_{n_i}) is. As mentioned above, the onset of the photon burst can be avoided by exchanging the population between levels, thereby sending the time *backwards* until the next onset of the photon burst phase at which point another exchange of population is executed. In Ref. [10] the application of a π pulse was suggested as a means of achieving this population

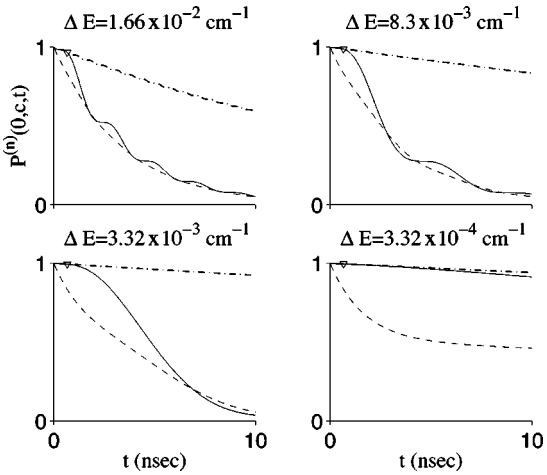

FIG. 5. Suppression of the $2P$-$1S$ spontaneous emission in the hydrogen atom, for which the natural linewidth is $\hbar\Gamma=1.66\times10^{-3}$ cm^{-1}. The solid lines display the decay of the optimized superposition of the Autler-Townes split levels with no interruptions. The dot-dashed lines are the decay curves of the same superposition states in the presence of interruptions. The dashed lines display the average decay of the two Autler-Townes split components. The optimization time τ (marked by a triangle) is $0.2/\Gamma=0.65$ ns, and the total time range displayed is 0 to $3/\Gamma=10$ ns.

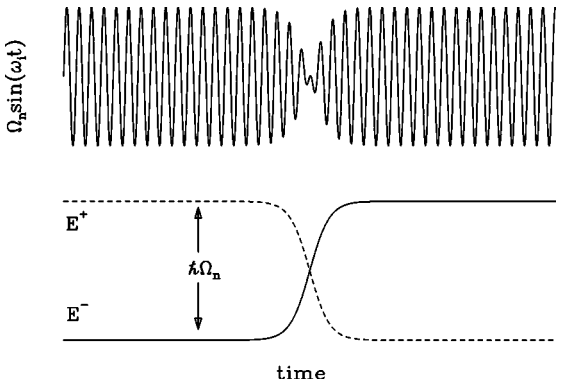

FIG. 6. The train wave of the spectator cw field of frequency ω_i near an interruption which switches Ω_{n_i} to $-\Omega_{n_i}$, thereby exchanging the order of the $E^{\pm}_{n_i}$ levels, as shown in the lower panel.

exchange. However, because in atoms and homonuclear diatomic molecules the $|+n_i,0\rangle$ and $|-n_i,0\rangle$ states are not coupled optically to one another, the π pulse in question would have to arise from a two-photon (e.g., Raman) process. Rather than do this we can within the framework of the present setup achieve the same reversal of time by switching the levels while keeping the population of the levels intact. According to Eq. (23), we can switch the order of the $E^{\pm}_{n_i}$ levels by adiabatically changing the sign of Ω_{n_i}. A schematic illustration as to the kind of interruption needed in the spectator cw field to achieve this is displayed in Fig. 6.

The result of the kind of interruptions displayed in Fig. 6 is shown as the dot-dash curve of Fig. 5. We see that the spontaneous emission has been effectively suppressed, with the suppression becoming more effective, the smaller is the Autler Townes splitting. Also shown in Fig. 5 (as the dashed line) are the natural decay curves, arising when we start with one of the eigenstates, i.e., $c_{\alpha'}=\delta_{\alpha,\alpha'}$. As can be seen, this decay, which is *nonexponential* due to the interaction between the resonances, is still much faster than the suppressed decay aided by the interruptions.

B. Suppression of the spontaneous emission in the Pb atom

We now show that the above method works equally well in the presence of more than one final state to which the system can emit. We study the Pb atom and take as the $|a\rangle$ state the $6p\ 7s\ ^3P_1^0$ excited state which emits [21] to the

$$|1\rangle = 6p^2\ ^3P_0 \quad \lambda_1 = 283.31 \text{ nm} \quad A_{a,1} = 43.0 \ \mu\text{s}^{-1},$$

$$|2\rangle = 6p^2\ ^1P_1 \quad \lambda_2 = 363.96 \text{ nm} \quad A_{a,2} = 32.0 \ \mu\text{s}^{-1},$$

$$|3\rangle = 6p^2\ ^3P_2 \quad \lambda_3 = 405.79 \text{ nm} \quad A_{a,3} = 93.1 \ \mu\text{s}^{-1},$$

$$|b\rangle = 6p^2\ ^1D_2 \quad \lambda_4 = 722.90 \text{ nm} \quad A_{a,b} = 2.6 \ \mu\text{s}^{-1}$$

final states. The total decay rate of state $|a\rangle$ is therefore given as

$$\Gamma_{aa}(E_a) = \sum_{\gamma=1,2,3,b} a_{\alpha\gamma} = 171 \ \mu\text{s}^{-1}. \tag{44}$$

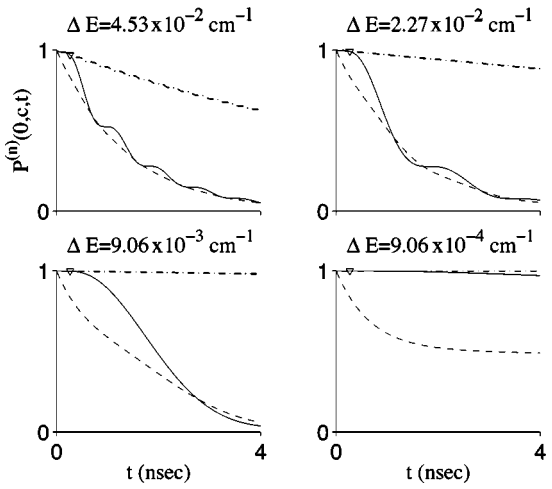

FIG. 7. Suppression of the spontaneous emission in the Pb atom, details are as in Fig. 5. The optimization time τ (marked by a triangle) is $0.2/\Gamma = 2.4$ ns, and the total time range displayed is 0 to $3/\Gamma = 35$ ns.

We assume that the decay rate of $|b\rangle$ is negligible compared with that of $|a\rangle$, hence, $\hbar\Gamma_{++}=\hbar\Gamma_{--}=\hbar\Gamma_{+-}=\frac{1}{2}\Gamma_{a,a}=4.531\times10^{-3}$ cm^{-1}. We note that $|a\rangle$ can decay to $|b\rangle$ as well as to the other states noted above.

The suppressed and natural decay curves for this system are shown in Fig. 7. We see that the suppression works extremely well, in fact better than in hydrogen, especially at the small splitting end.

C. Suppression of the $Na_2(A\rightarrow X)$ spontaneous emission

We now show that the above suppression of the spontaneous emission method works equally well for a molecular system. In molecular systems there is usually a *multitude* of final states to which the system can emit. In this example we consider suppressing the emission from a particular ($|a\rangle$) vibrational state belonging to the $1\ ^1\Sigma_u$ (A) electronic manifold, aided by a particular vibrational ($|b\rangle$) state belonging to the $2\ ^1\Sigma_g$ electronic manifold. The relevant potentials are displayed in Fig. 8.

Using an average electronic transition-dipole moment μ_e of 7 Debye ($=2.756$ a.u.) between the $1\ ^1\Sigma_u$ (A) and the ground $1\ ^1\Sigma_g$ (X) states [22], we have calculated the dipole moment matrix elements within the the Franck-Condon approximation, according to which

$$\mathbf{D}_{\nu,\gamma} \approx \mu_e \langle \nu | \gamma \rangle, \tag{45}$$

where $|\nu\rangle$ and $|\gamma\rangle$ signify vibrational states.

The vibrational wave functions needed for this calculation were derived from the potential energy curves of Schmidt [23]. In the present rough treatment only the vibrational states (without the rotational sublevels) were included in the calculations. The inclusion of the rotational factors is not expected to qualitatively change the conclusions drawn here.

The line shapes for the vibrational levels (and specifically that of $\nu=20$) of the excited surface $1\ ^1\Sigma_u$ are much nar-

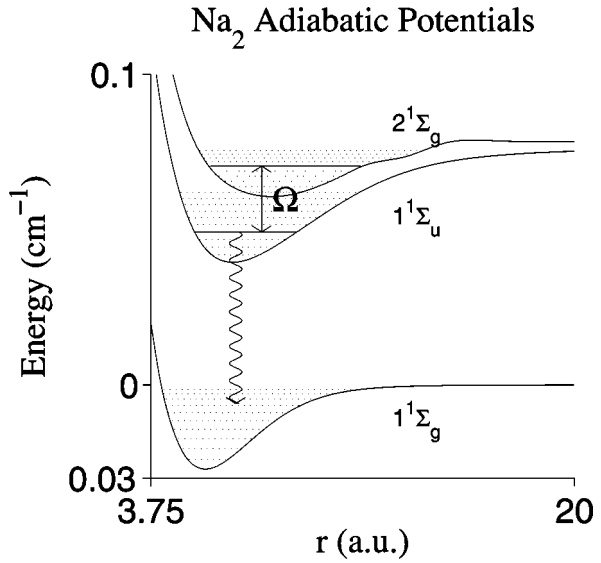

FIG. 8. The three lowest singlet potential-energy curves of Na_2: $1\,^1\Sigma_g$, $1\,^1\Sigma_u$, and $2\,^1\Sigma_g$. Every fifth vibrational level is marked with a dashed line. The $|a\rangle$ state is the $\nu=20$ vibrational level of the second potential. The $|b\rangle$ state is the $\nu'=30$ vibrational level of the third potential. Both are marked by solid lines. The Franck-Condon factor (equal to overlap integral) between these two states is 0.118.

rower than the energy level spacing, therefore all the resonances are isolated, as in the atomic cases discussed above.

Assuming that the decay rates of the vibrational levels belonging to the $2\,^1\Sigma_g$ manifold (which can decay to the $1\,^1\Sigma_u$ manifold) are negligible compared to those of the $1\,^1\Sigma_u$ surface, we can write $\Gamma_{\nu\nu}(E)$ as

$$\Gamma_{\nu\nu}(E)=\frac{e^2}{3\pi\varepsilon_0\hbar^4c^3}\sum_{\{\gamma:E>E_\gamma\}}|\mathbf{D}_{\nu,\gamma}|^2(E-E_\gamma)^3, \quad (46)$$

where γ includes only the vibrational levels in the ground electronic manifold. We obtain for $0\leqslant\nu\leqslant30$, $\Gamma_{\nu\nu}(E_\nu+n_i\hbar\omega_i)\approx40\ \mu s^{-1}$ or $\hbar\Gamma_{\nu\nu}=2.12\times10^{-4}\ \mathrm{cm}^{-1}$. The change of $\Gamma_{\nu\nu}(E)$ with energy may be neglected, since the

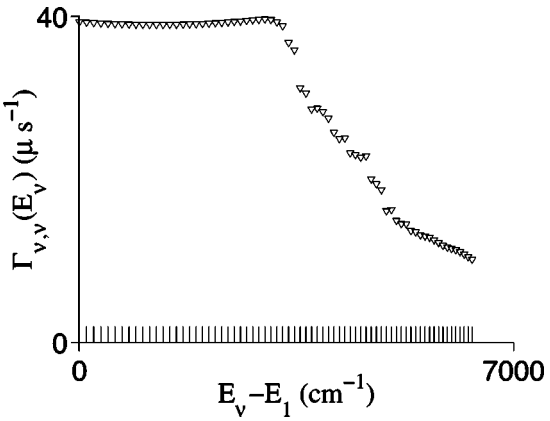

FIG. 9. The decay rates $\Gamma_{\nu\nu}(E_\nu+n_i\hbar\omega_i)$ of the 70 lowest vibrational states $|\nu\rangle$ of the $1\,^1\Sigma_u$ surface.

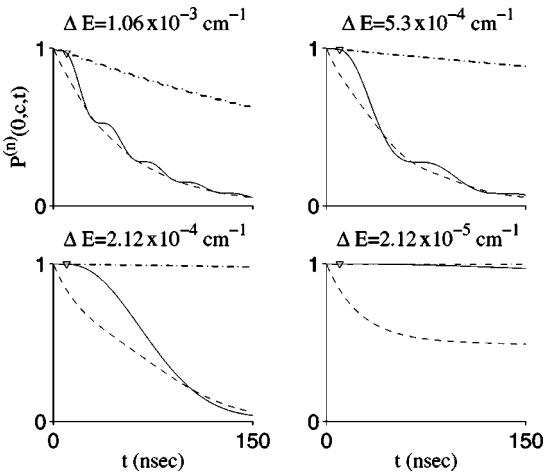

FIG. 10. Suppression of the spontaneous emission of the sodium dimer. The optimization time τ (marked by a triangle) is $0.2/\Gamma=10$ ns, and the total time range displayed is 0 to $3/\Gamma=150$ ns.

relevant integration range around E_ν, $\pm\hbar\Gamma=\pm2.1\times10^{-4}\ \mathrm{cm}^{-1}$, is much smaller than $E_\nu-E_\gamma$ for *all* $|\gamma\rangle$ ground states considered.

Figure 9 displays the decay widths $\Gamma_{\nu\nu}(E_\nu)$ for the 70 lowest vibrational states $|\nu\rangle$ of the $1\,^1\Sigma_u$ surface. Also displayed are the energy levels E_ν.

The decay curves resulting from coupling the $|a\rangle=|\nu=20\rangle$ with the $|b\rangle=|\nu'=30\rangle$ are shown in Fig. 10. Again the method is very successful in completely suppressing the decay.

IV. CONCLUSIONS

We have presented an experimentally viable approach for suppressing the spontaneous emission in a number of realistic systems. In this method a single resonance is split by an external (spectator) field, and an optimized superposition of the two components is formed by a shaped pulse excitation from the ground state. We have shown that by introducing infrequent phase interruptions we can completely (or almost completely) suppress the spontaneous emission in the H atom, the Pb atom, and the Na_2 molecule.

In addition, we have introduced a number of improvements over our original method [10], which are (1) the ability to work with isolated resonances; (2) the ability to tune ΔE, the spacing between the split components, by varying the cw field intensity, thereby stretching or contracting the duration of the ''quiescent'' phase; (3) the ability to completely suppress the decay by introducing phase jumps, or electric-field sign reversals, in the spectator field which causes the Autler-Townes splitting. This interruption method is expected to be much easier to apply in the laboratory than our previous suggestion of applying a (Raman) π pulse, which would have necessitated the introduction of two additional laser fields.

ACKNOWLEDGMENTS

This project was supported by the Minerva Foundation, GIF, and the EU IHP program HPRN-CT-1999-00129.

[1] B. Misra, J. Math. Phys. **18**, 756 (1977).
[2] G.J. Milburn, J. Opt. Soc. Am. B **5**, 1317 (1988).
[3] W.M. Itano, D.J. Heinzen, J.J. Bollinger, and D.J. Wineland, Phys. Rev. A **41**, 2295 (1990).
[4] P. Knight, Nature (London) **344**, 493 (1990).
[5] V. Frerichs and A. Schenzle, Phys. Rev. A **44**, 1991 (1962).
[6] A.G. Kofman and G. Kurizki, Phys. Rev. A **54**, R3750 (1996).
[7] P. Facchi and S. Pascazio, Phys. Lett. A **241**, 139 (1998).
[8] A.G. Kofman and G. Kurizki, Nature (London) **405**, 546 (2000).
[9] M.B. Plenio, P.L. Knight, and R.C. Thompson, Opt. Commun. **123**, 278 (1996).
[10] E. Frishman and M. Shapiro, Phys. Rev. Lett. **87**, 253001 (2001).
[11] S.H. Autler and C.H. Townes, Phys. Rev. **100**, 703 (1955).
[12] K.C. Friedrichs, Commun. Pure Appl. Math. **1**, 361 (1948).
[13] H. Feshbach, Ann. Phys. (N.Y.) **19**, 287 (1962); **43**, 410 (1967).
[14] U. Fano, Phys. Rev. **124**, 1866 (1961).
[15] R.D. Levine, *Quantum Mechanics of Molecular Rate Processes* (Clarendon Press, Oxford, U.K., 1969).
[16] M. Shapiro, J. Chem. Phys. **56**, 2582 (1972).
[17] S.E. Harris, Phys. Rev. Lett. **62**, 1033 (1989).
[18] C. Cohen-Tannoudji, B. Diu, and F. Laloë, *Quantum Mechanics* (Wiley, New York, 1977).
[19] M.O. Scully and M.S. Zubairy, *Quantum Optics* (Cambridge University Press, Cambridge, 1997).
[20] R. Loudon, *The Quantum Theory of Light*, 2nd ed. (Claredon, Oxford, 1983), Eqs. 4.111, 4.113, 5.140, pp. 174–179.
[21] A. Alonso-Medina, J. Quant. Spectrosc. Radiat. Transf. **55(2)**, 151 (1996).
[22] W.J. Stevens, M.M. Hessel, P.J. Bertonicini, and A.C. Wahl, J. Chem. Phys. **66**, 1477 (1977).
[23] The Na-Na potential curves and the relevant electronic dipole moments are from I. Schmidt, Ph.D. thesis, Kaiserslautern University, 1987.